CHINESE JOURNAL OF MECHANICAL ENGINEERING
Vol. 27, No. 4, 2014

DOI: 10.3901/CJME.2014.0421.079, available online at www.springerlink.com; www.cjmenet.com; www.cjmenet.com.cn

Transient-Spatial Pattern Mining of Eddy Current Pulsed Thermography Using Wavelet Transform

YANG Hailong[1], GAO Bin[1, *], TIAN Guiyun[1, 2], REN Wenwei[1], and WOO Wai Lok[2]

1 *School of Automation Engineering, University of Electronic Science and Technology of China, Chengdu 611731, China*
2 *School of Electrical and Electronic Engineering, Newcastle University, UK*

Received December 19, 2013; revised April 17, 2014; accepted April 21, 2014

Abstract: Eddy current pulsed thermography(ECPT) is an emerging Non-destructive testing and evaluation(NDT & E) technique, which uses hybrid eddy current and thermography NDT & E techniques that enhances the detectability from their compensation. Currently, this technique is limited by the manual selection of proper contrast frames and the issue of improving the efficiency of defect detection of complex structure samples remains a challenge. In order to select a specific frame from transient thermal image sequences to maximize the contrast of thermal variation and defect pattern from complex structure samples, an energy driven approach to compute the coefficient energy of wavelet transform is proposed which has the potential of automatically selecting both optimal transient frame and spatial scale for defect detection using ECPT. According to analysis of the variation of different frequency component and the comparison study of the detection performance of different scale and wavelets, the frame at the end of heating phase is automatically selected as an optimal transient frame for defect detection. In addition, the detection capabilities of the complex structure samples can be enhanced through proper spatial scale and wavelet selection. The proposed method has successfully been applied to low speed impact damage detection of carbon fibre reinforced polymer(CFRP) composite as well as providing the guidance to improve the detectability of ECPT technique.

Keywords: non-destructive testing and evaluation, composite impact damage detection, wavelet transform, energy driven approach, transient-spatial analysis

1 Introduction

Carbon fibre reinforced polymer(CFRP) composite is widely used in many areas such as aircraft and wind turbine blades because of its low weight and high strength. Therefore, the safety guarantee of using this composite is extreme important for research field in Non-destructive Detection and Evaluation(NDT & E)[1–2]. Impact damage is one of the most common types of composite related defect, which often results in the operational failure of system. In recent years, many NDT & E techniques are developed such as ultrasonic testing[3–4], eddy current[5–6], acoustic emission[7], thermography[8–9], microwave[10], X-ray[11] and computer tomography(CT)[12] for CFRP composites defect detection.

Eddy current pulsed thermography(ECPT) is an emerging NDT & E technique, which combine eddy current and thermography NDT & E techniques that enhance the detectability from their compensation[13–15]. ECPT applies high current electromagnetic pulse to the conductive material under inspection which the heat is not limited to the sample surface, rather it can reach a certain depth, which governed by the skin depth of eddy current. This is different from other thermography based NDT techniques such as flash and laser thermographies that mainly introduce heat at the surface. In addition, ECPT has the ability of adaptability in terms of defect orientation and can enhance specific excitation direction to optimize the directional evaluation along the defect orientation, which is more effective for geometrically complex components and illustrated more crack indication. Furthermore, ECPT allows area imaging of defects without scanning and enable users to detect both magnetic and non-magnetic metals. ECPT has been applied into many studies including the potential for small defect detection of complex geometry estimating the fatigue cracks in steel[16] as well as an investigation of temperature distribution around cracks with different penetration depths in metallic materials[17]. Another study has examined in detection of multiple cracks from rolling contact fatigue in rail tracks with a single measurement[18]. Quantitative NDE(QNDE) at a pixel level has been reported in previous PEC work and can help derive multiple properties of materials[19]. Once the thermography video has been obtained, various signal processing techniques can be used to extract features to

* Corresponding author. E-mail: bin_gao@uestc.edu.cn
Supported by National Natural Science Foundation of China(Grant No. 51377015), China Post Doctor Project(Grant No. 136413), and Science & Technology Department of Sichuan Province, China(Grant No. 2013HH0059)

qualify and quantify the defects detection[20]. To enhance the flaw contrast and improve noise rejection qualities, pattern based image sequences processing has been conducted by introducing the raw data upon a set of orthogonal basis functions. Principal component analysis (PCA) and independent component analysis(ICA)[21–24] based pattern extraction algorithms are used to improve the flaw detectability of thermography by considering the initial sequences as either a set of images or a set of temporal profiles.

Compare to defects in metal, those in composite materials were rarely investigated. REN, et al[25], proposed optical flow based methods to track both temperature spatial and transient diffusion and use divergence to quantify the degree of impact damage of CFRP. HE, et al[26], used Fourier transform based frequency pattern extraction methods and project thermal signal phase map to enhance the flaw-contrast and reduce the emissivity. Manually pixel selection and signal normalized based processing method[27] to analysis of notches in CFRP material is evaluated and used to quantify depth information of defects. BUI, et al[28], dedicated to an accurate model of the stratified CFRP composite material and an original NDT technique for detection and characterization of the delamination and fiber rupture. GUO, et al[29], carried out image reconstruction methods based on logarithm polynomial regression to reconstruct and enhance pulsed thermography(PT) image sequences of CFRP laminates.

All the above defect detection methods of composite are limited by the manual selection of proper contrast frames or investigated area. In addition, they work well only if the damaged sample caused by larger impact energy. However, the identification and location of low energy impact damage is still a challenge task for composite defect detection when using ECPT. The information of impact damage is significantly influenced and difficult to be identified because of the complexity construction of composite material such as non-homogeneous and inter-crossed fibre structure. In ECPT, the transient temperature response is a time dependent signal, including heating phase and cooling phase. Different time interval contains different physical effects. Besides the manual selection, it is critical to develop an automatic method which enables us to select a proper time interval for enhancing the defect detectability. Therefore, automatic transient selection and the optimized defect identification methods are required. Wavelet transform have been found to be effective in time, frequency and spatial analysis and its function as a mathematical microscope of signal analysis for many image processing based applications[30–32] such as image compression, de-noising, and etc. In this paper, we have proposed wavelet coefficient energy driven based automatic transient-spatial selective method to strengthen the micro impact damage detection and optimize the selection of transient interval. The foundation for the proposed method is specified. Experimental tests on low energy impact CFRP samples have been conducted to show the validation of the pattern extraction. The rest of the paper is organized as follows. Section 2 introduces the proposed spatial-transient optimization methodology of ECPT. The experimental system and analysis are illustrated in section 3. The conclusion and future work are presented in section 4.

2 Methodology

There are several different time frequency analysis methods[33] such as short time Fourier transform(STFT) and wavelet transform(WT). The STFT decomposes a time signal into a time-frequency(TF) domain, and variations of the frequency within the window function are revealed. STFT has an equal-spaced bandwidth across all frequency channels. Wavelet transform is a tool that converts a signal into a non-uniform TF resolution, which is more suitable for analyzing non-stationary and non-periodic signal. Wavelet is a small wave that has an oscillating wavelike characteristic and has its energy concentration in time. In contrast to STFT, the wavelet transform enables variable window sizes in analyzing different frequency components within a signal. By comparing the signal with a set of functions obtained from the scaling and shift of a base wavelet. Wavelet analysis is a subject which has significance in both theory and application. Both continuous wavelet transform(CWT) and discrete wavelet transform(DWT) have been found to be effective approaches in many applications, especially in the case of two-dimensional signal. In addition to microscopic capability, wavelet analysis also has the ability of polarization. As thermal image signal is highly non-stationary and non-periodic, the time-frequency analysis of using wavelet transform of ECPT image sequences is studied. In mathematics, the definition of continuous wavelet transform as in Eq. (1):

$$\boldsymbol{X}(\tau,i)=\frac{1}{\sqrt{i}}\int_{-\infty}^{\infty}X(t)\psi\left(\frac{t-\tau}{i}\right)\mathrm{d}t, \tag{1}$$

where τ shifts time, i modulates the width, and $\psi(t)$ is mother wavelet. CWT has the superposition property and has its unique advantages in signal processing such as pattern recognition, feature extraction and detection. There are several commonly used wavelets for performing the CWT such as mexical hat, molert, Frequency B-Spline Wavelet, Shannon Wavelet, Gaussian Wavelet, Harmonic Wavelet, and etc. DWT is another form of WT which involves the use of the dyadic scheme. This satisfied by the utilisation of discrete value of the scaling and translation, $i=2^{\beta}$, $\tau=\varepsilon 2^{\beta}$, ε, $\beta\in\mathbf{Z}$, where $\mathbf{Z}$ denotes the set of integers. Different decomposition levels corresponding to different scales(wavelet width) and time shift in DWT. DWT has

been widely used in image processing such as image filtering, compressing, and etc. Because DWT can achieve orthogonal decomposition of the signal and enable to divide signal into nonoverlapping subfrequency bands effectively, that means it is more of interest in the context of fast, nonredundant transforms and has less computation complexity. DWT also provides a compact representation of a signal's frequency components with strong spatial support and enable to decompose a signal into frequency subbands at different scales from which it can be perfectly reconstructed. Thus, in this study, DWT is utilized to analysis the thermal image sequences. When applying DWT to ECPT image, wavelet coefficient at each level are obtained. The more similar these wavelets are to the signal components, the larger the wavelet coefficients. In each scale level, the detail information of signal distributed within these frequency bands can be further processed to extract defect related components.

2.1 Flow chart of the proposed method

The specific signal processing and optimization procedure diagram, which illustrates the relationship of transient selection, scale selection and wavelet selection are shown in Fig. 1.

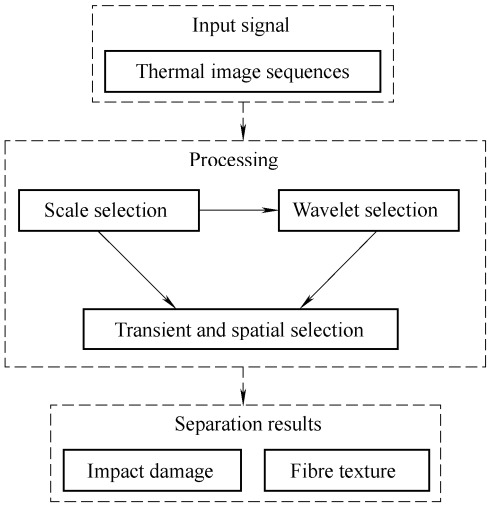

Fig. 1. Procedure diagram proposed

In Fig. 1, the specific procedure of the proposed method can be summarized as the following steps.

Step 1: Input raw thermal sequences from ECPT.

Step 2: Optimize the scale through comparing the mean coefficient energy of multi-level wavelet transform and find the scale where it enable to maximize the separability for fibre and impact thermal patterns.

Step 3: Select optimal wavelet through applying the maximum energy criteria under the selected scale.

Step 4: Select optimal transient frame through abserving the variation of low and high frequency components with the change of time at the selected scale using the optimal wavelet.

Step 5: Use the optimal wavelet and selected scale to do wavelet transform to the optimized transient ECPT image.

Step 6: Detect the impact damage and fibre texture information.

2.2 Proper transient frame selection of ECPT

The behave of thermal transient on tested sample can be recorded during ECPT and the most of current methods mainly manually select a specific transient frame to detect and quantify the defects. However, the drawbacks of current methods originate from its lack of a generalized criterion for selecting proper transient frame to maximize the detectability for defects. In practice, these methods will inevitably suffer from under-informative which subsequently lead to ambiguity in the defect detection. In this paper, we initialize the *i*th level DWT(the *i*th level denotes decomposition level of using DWT. More discussion of proper level selection will be discussed in section 2.3).

Fig. 2 presents the procedure of using discrete wavelet transform to analyze the time frequency component for whole transient frames $\{\boldsymbol{X}(t)\}_{t=1}^{N}$, where $t=1, 2,\cdots, N$. $\boldsymbol{X}(t)$ denotes transient frame at t time point. N denotes the total frames.

The richness of using 2D wavelet transform guarantees the decomposition covers all directions (horizontal, vertical and diagonal). Therefore, the decomposition results will likewise cover all directions even without knowing the fiber orientations. The *i*th level coefficient matrix of DWT for approximation, detail (horizontal, vertical and diagonal) can be expressed by Eqs.(2)–(5):

$$\boldsymbol{Y}_A^i(t)=\mathrm{DWT}_A^i\{\boldsymbol{X}(t)\}, \tag{2}$$

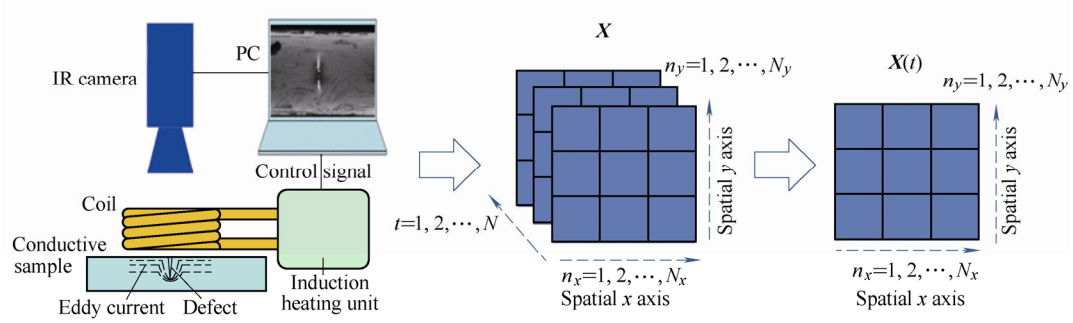

Fig. 2. ECPT schematic and transient frame sequences

$$\boldsymbol{Y}_H^i(t) = \mathrm{DWT}_H^i\left\{\boldsymbol{X}(t)\right\}, \tag{3}$$

$$\boldsymbol{Y}_V^i(t) = \mathrm{DWT}_V^i\left\{\boldsymbol{X}(t)\right\}, \tag{4}$$

$$\boldsymbol{Y}_D^i(t) = \mathrm{DWT}_D^i\left\{\boldsymbol{X}(t)\right\}, \tag{5}$$

where $\boldsymbol{X}(t)$ denotes thermal image, $\boldsymbol{Y}_A^i(t)$, $\boldsymbol{Y}_H^i(t)$, $\boldsymbol{Y}_V^i(t)$, $\boldsymbol{Y}_D^i(t)$ denotes ith decomposition level of approximation, horizontal, vertical and diagonal detail wavelet coefficient matrix, respectively. Here $\boldsymbol{Y}_A^i(t)$, $\boldsymbol{Y}_H^i(t)$, $\boldsymbol{Y}_V^i(t)$, $\boldsymbol{Y}_D^i(t)$ are matrix with dimension of $J\times K$. $\mathrm{DWT}^i\{\bullet\}$ denotes the discrete wavelet transform at the ith level.

After the coefficient matrix at ith level was obtained, the coefficient energy of different thermal images was computed and compared. The approximation and horizontal, vertical, diagonal detail coefficient energy was calculated by Eqs. (6)–(9):

$$E_A^i(t) = \sum a_{j,k}^2, \tag{6}$$

$$E_H^i(t) = \sum h_{j,k}^2, \tag{7}$$

$$E_V^i(t) = \sum v_{j,k}^2, \tag{8}$$

$$E_D^i(t) = \sum d_{j,k}^2, \tag{9}$$

where $E_A^i(t)$, $E_H^i(t)$, $E_V^i(t)$, $E_D^i(t)$ denotes approximation and horizontal, vertical diagonal detail coefficient energy of $\boldsymbol{X}(t)$ at the ith level, respectively. $a_{j,k}$, $h_{j,k}$, $v_{j,k}$, $d_{j,k}$ is the (j,k)th element of coefficient matrix $\boldsymbol{Y}_A^i(t)$, $\boldsymbol{Y}_H^i(t)$, $\boldsymbol{Y}_V^i(t)$, $\boldsymbol{Y}_D^i(t)$, respectively.

Through Eqs. (6)–(9), the approximation and detail coefficient energy in different direcion at ith level of all transient images was calculated. Once the coefficient energy at ith level of all frames was calculated, the coefficient energy of different frames was compared and the elbow point is chosen in which can balance the richness of informative for both low and high frequency component as being considered as the optimal transient selection. More discussion and analysis will be specified in section 3.2.

2.3 Proper spatial scale selection

Once the proper transient frame has been selected, the target is to enhance the spatial resolution of defect identification. As mentioned in section 2.2, different frequency component can be extracted from the transient image through changing the scale of WT. This is performed by stretching and translating the mother wavelet via varying the scale index. Therefore, the more similar these wavelets are to the signal components, the larger the wavelet coefficients. This means the wavelet coefficients will have relatively high magnitudes for the case where a high correlation between a major frequency components corresponding to a particular component exists in the signal. This correlation can be judged by computing the mean coefficient energy and the proper scale can be selected. In this study, the optimal scale selection focus on the analysis of different decomposition level, which has the potential to maximize the separability of fibre and impact thermal patterns. Because the dimension of coefficient matrix was halved after each decomposition level, thus the mean coefficient energy at different level was computed and compared to get fair level selection. Namely

$$e_A(i) = \sum a_{j,k}^2 / (J\times K), \tag{10}$$

$$e_H(i) = \sum h_{j,k}^2 / (J\times K), \tag{11}$$

$$e_V(i) = \sum v_{j,k}^2 / (J\times K), \tag{12}$$

$$e_D(i) = \sum d_{j,k}^2 / (J\times K), \tag{13}$$

where $e_A(i)$, $e_H(i)$, $e_V(i)$, $e_D(i)$, denotes the mean coefficient energy at ith decomposition level, respectively. $a_{j,k}$, $h_{j,k}$, $v_{j,k}$ $d_{j,k}$ is the (j,k)th element of coefficient matrix $\boldsymbol{Y}_A^i(t)$, $\boldsymbol{Y}_H^i(t)$, $\boldsymbol{Y}_V^i(t)$, $\boldsymbol{Y}_D^i(t)$, respectively. $j = 1,2,\cdots,J$, $k = 1,2,\cdots,K$, $J\times K$ is the dimension of coefficient matrix.

2.4 Mother wavelet selection

The key to the use of WT is to look for a set of different base wavelets. Base wavelets are characterized by orthogonality, symmetry and compact support. Understanding these properties will be helpful to choose a candidate base wavelet from the wavelet families for analyzing different signals. For example, the orthogonality property indicates that the inner product of the base wavelet is unity with itself, and zero with other scaled and shifted wavelets. As a result, an orthogonal wavelet is efficient for signal decomposition into nonoverlapping subfrequency bands. The symmetric property ensures that a base wavelet can serve as a linear phase filter. A compact support wavelet is the one whose basis function is nonzero only within a finite interval. This allows the wavelet transform to efficiently represent signals that have localized features.

There are two ways to measure wavelet performance, one is qualitative and the other is quantitative. Qualitative criteria like shape matching. As far as shape matching is concerned, it is generally difficult to accurately match the shape of a signal to that of a base wavelet through a visual comparison. These deficiencies motivate the study of quantitative measures for base wavelet selection.

Quantitative criteria like maximum cross correlation coefficient between the wavelets and the signal under analysis. Furthermore, there are two more quantitative criteria to determine optimal wavelet base, which are maximum energy and minimum Shannon Entropy.

In this study, the maximum energy criteria was proposed to select a optimal base wavelet. The energy content of a signal $X(t)$ can be calculated by Eq. (14):

$$E = \int |X(t)|^2 \, \mathrm{d}\tau. \tag{14}$$

Simultaneously, it can be calculated from its wavelet coefficients WT(i, τ):

$$E = \iint |\mathrm{WT}(i,\tau)|^2 \, \mathrm{d}i\mathrm{d}\tau. \tag{15}$$

The ith level energy can be revised as

$$E^i = \int |\mathrm{WT}(i,\tau)|^2 \, \mathrm{d}\tau. \tag{16}$$

In practical, the wavelet coefficients is discrete, thus the energy content of the signal at the scale i of DWT can be approximately measured by Eq. (17):

$$E^i = \sum \{\mathrm{DWT}(i,\tau)\}^2. \tag{17}$$

The optimal wavelets are those most close to the signal under analysis. The more closer the wavelets are to the signal, the magnitude of wavelet coefficient will be larger. The reason is because a specific frequency energy content of a signal can be reflected from the wavelet coefficient at a specific scale and the ideal base wavelet that can extract the largest amount of energy from the signal at the selected scale.

3 Experiment and Analysis

3.1 Experimental set-up and sample preparation

ECPT system including excitation source, induction coil and a thermal camera is shown in Fig. 3. An Easyheat 224 from Cheltenham Induction Heating is used for coil excitation to generate a maximum current of 400 A_{rms} and an excitation frequency range of 150–400 kHz(380 A and 256 kHz are used in the experiments) with a maximum excitation power of 2.4 kW. In general, high excitation frequencies will lead to different skin depths and a high induced temperature due to eddy current heating. The time-domain thermal information will be used to derive defect profile information. The Flir SC7500 is a Stirling cooled camera with a 320×256 array of 1.5–5 μm InSb detectors. The camera has a sensitivity of <20 mK and a maximum full frame rate of 383 Hz. A video comprising of 191 frames of transient thermal images showing impact damage of the CFRP sample with pulse thermography can be retrieved using this system.

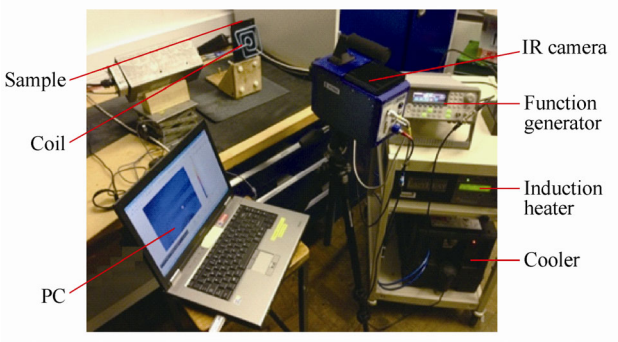

Fig. 3. ECPT system setup

The impact damage was manufactured in the middle of the sample by a small impact energy of 4 J using CEAST FractovisPlus 9350 impaction equipment. The impactor is hemi-spherical 22.2 mm in diameter and a mass of 2.04 kg. The impacts were produced under conditions specified by ASTM D7136 at a temperature of 20±10℃. Fig. 4 shows the impact damage schematic.

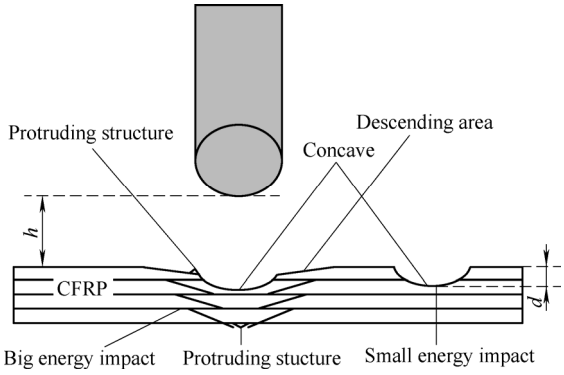

Fig. 4. Impact damage schematic

The sample was produced by TenCate Advanced Composites, Netherlands, and provided by Prof. Raimond Grimberg from National Institute of Research and Development for Technical Physics, Romania. The 4J impacted test sample is shown in Fig. 5.

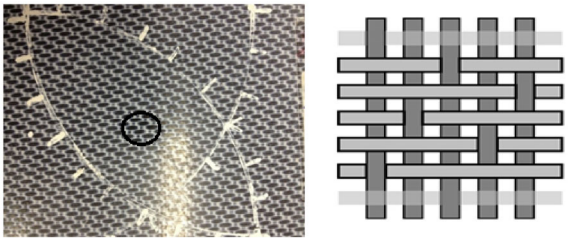

(a) Image of impacted sample (b) Structure of fibre

Fig. 5. Image of impacted sample and structure of fibre

The ECPT thermal video of 4J impact damage where impact point is marked as circle box in Fig. 5(a) is provided by Newcastle University. There are two modes for ECPT equipment to produce transient thermal image. One is reflection mode, and the other is transmission mode. Because thermal image sequences in reflection mode was blocked by the induction coil, which then influence the later analysis. In this study, the transmission mode was applied.

3.2 Impact of transient selection

As mentioned in section 2, the coefficient energy of DWT in different decomposition level can reflect the frequency component of the signal. In this study, the coefficients at fourth level from DWT was chosen because both fibre and impact thermal informative patterns are approximate fully separated. More discussion on level selection will be detailed in Section 3.3. In order to find the optimal transient frame, coefficient energy of both low and high frequency components are computed and compared among all frame sequences. As 2D WT is directional which means the decomposition covers different directions such as horizontal, vertical, diagonal, DWT decomposes image into four sub-matrixes where low frequency component serves as approximation and the other three high frequency (horizontal, vertical and diagonal) components reflect the details. In this study, for high frequency component, we select one direction as a representative because the distribution of details in all three directions behaves almost the same.

Since thermal image consists of low and high frequency component, it is expected to observe the variation of energy driving at both low and high frequency components along with the transient of thermal image sequences to select a proper frame. As can be seen from the Fig. 6, the variation of coefficient energy of approximation component and detail component are different. The energy of low frequency component increases with constant speed to an elbow point, and then remain a steady state rate. The energy of high frequency component performs completely different where it has a high rising rate to the same elbow point and then decreases sharply to the bottom. These phenomena can be explained from a physical point of view. In the composites, fibre-woven construct together and resin as a supporting body. Macroscopic observations found that[25], the small impact energy can result in a concave imprint on the surface of specimen. This deformation will leads to accumulation of eddy current in this area. In heating phase, since the electrical and thermal conductivity is the greatest along the fibre orientation[34], the generated Joule heating increases the temperature along the fibre orientation rapidly. In the cooling phase, since there is no heating source, the heat diffusion[24] starts from the higher temperature areas(fiber) to the surrounding area. That is why the coefficient energy of fibre related high frequency component increase rapidly in the heating stage and decrease sharply at the cooling stage. Low-frequency component contains the majority energy of the ECPT image signal, which represents the heat generation and diffusion contour of the whole specimen. It increases in the heating stage and then with a slight rise because of heat diffusion from higher temperature areas(fibre) at the beginning of the cooling stage. This changing process is relatively stable and finally achieves a balance state. In this study, the elbow point as frame 76 was selected which balance the richness of informative for both low(impact detection) and high frequency component(fibre information) as being considered as the optimal transient selection. These two transient characteristics provide us with a signature to distinguish the impact and fiber component which can be used as features to recognize a diverse range of defects.

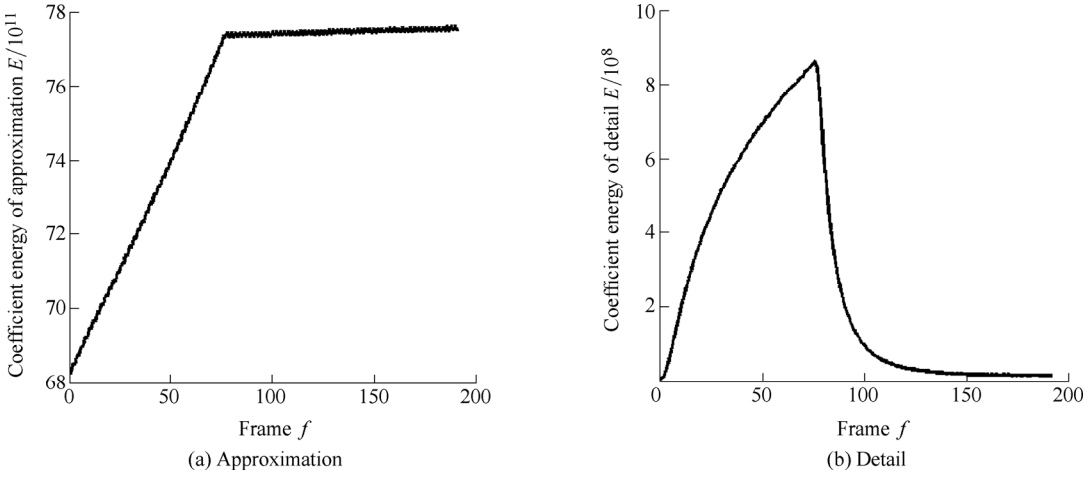

Fig. 6. Approximation and detail changes with the transient time

For validating the proposed transient selection method, we randomly choose other frames for comparison. Figs. 7 (a), (b), (c) compare the spatial resolution of impact detection using low frequency component by selecting different transient frames and Figs. 7(d), (e), (f) show fibre related thermal information(using H4 as a representative),

as it is another important phenomenon, which can be further analyzed for delamination and fiber rupture, and etc. As it can be seen from the Fig. 7, time point selection will impact the results. The fibre information can be clearly detected while the impact point cannot be seen in frame 50, the impact point in frame 120 is blurred because of the heat diffusion in the cooling stage and the fibre information is not very clear, while the impact damage and fibre information can both be seen clearly in frame 76. Through the comparison we learn that the selection of frame will influence the results and proper frame selection is needed. Frame 76 is selected as an optimal frame for further study.

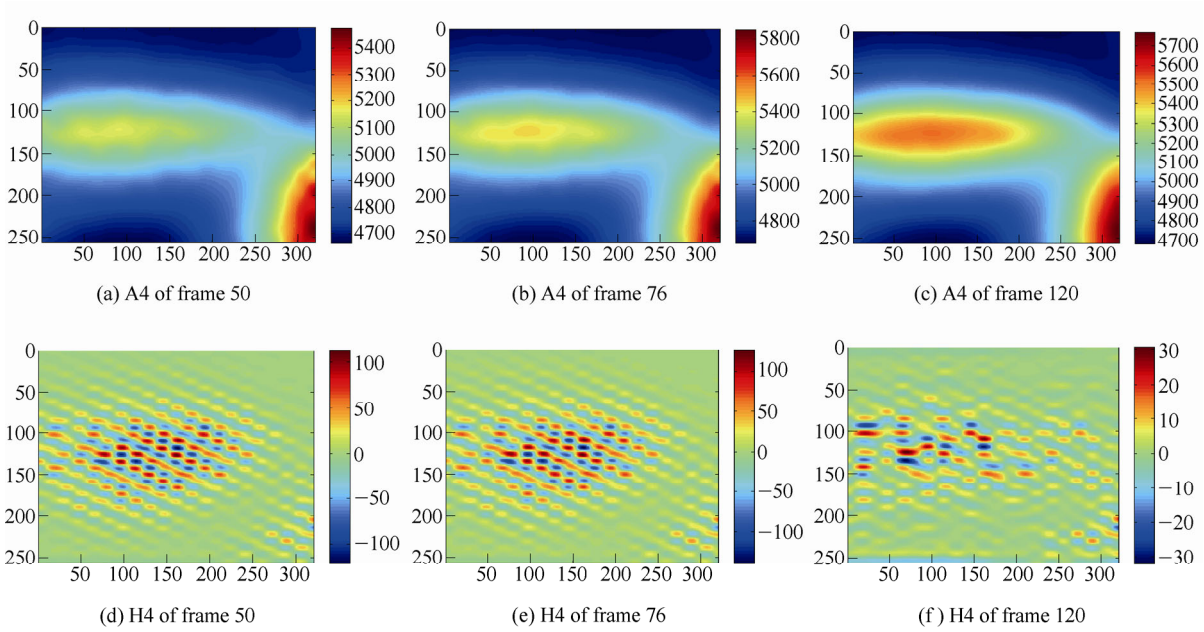

Fig. 7. Impact point and fibre detection and comparison by selecting different transient frame

3.3 Impact of spatial scale selection

Mean coefficient energy of I level WT decomposition was computed to select a proper scale of decomposition. The I=5 level decomposition results are shown in the Fig. 8.

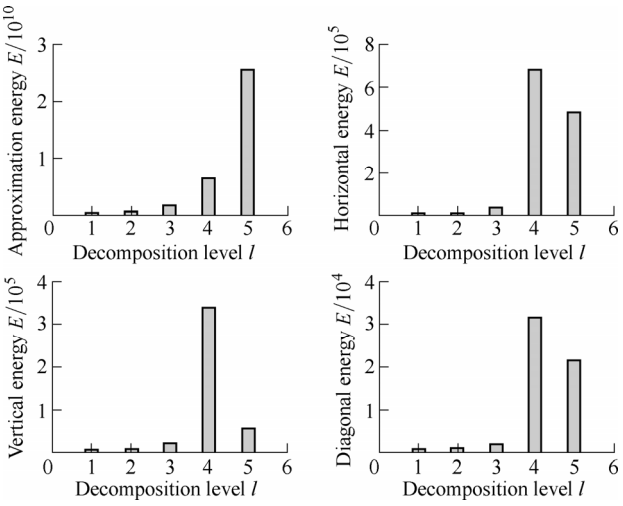

Fig. 8. Mean coefficient energy of each level, where horizontal axis represents decomposition level and vertical axis represents the mean coefficient energy value of each level

As can be seen from Fig. 8, the mean coefficient energy of the approximation increase gradually with the increase of decompositon level. However, the mean coefficient energy of the details(horizontal, vertical and diagonal) are very small at the first three levels, while the mean coefficient energy at the fourth level is the largest among the five level decomposition. That means a major frequency component corresponding to the scale of level four exists in the thermal image, then the wavelet coefficients at this level will have relatively high magnitudes. Thus, the components related to that scale can be extracted from the thermal image signal through the wavelet transform. Fig. 9 shows the five level decomposition and reconstruction results using the optimal wavelet (how to select a optimal wavelet will be detailed in section 3.4).

As can be seen from Fig. 9, after the reconstruction, part of high frequency components was filtered out from the thermal image in the first three level. However, the fibre information still exist in the approximation image. More precisely, the fourth level DWT leads to an approximately perfect separation of impact approximation and fibre details as compared to the other level of decomposition performance. This consistent with what has been discussed why the high frequency mean coefficient energy at fourth level is much larger than the other levels. In the study, the fourth level is selected as the proper decomposition level while the purpose to display 5-level decomposition results is to illustrate the performance comparison.Thus, the proper scale was selected which has the potential to maximize the separability of fibre and impact.

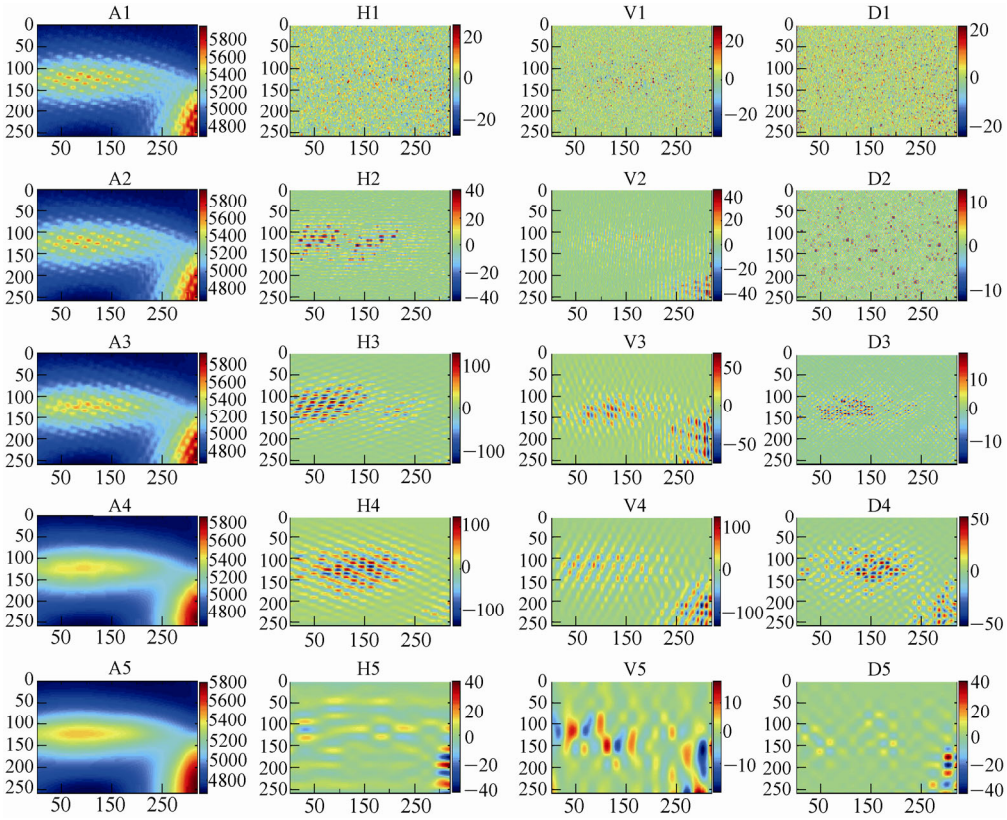

Fig. 9. Five level decomposition and reconstruction of frame 76

3.4 Impact of mother wavelet selection

In this section, we compare the performance of choosing different wavelets for decomposition. Through experiments, several suitable wavelet candidates are selected. They are db(5–10), coif(4–5), bior(3.5, 3.7, 3.9–6.8), sym(5–10).

Different base wavelet coefficients energy was computed and compared. The optimal wavelet is the one which extract the most energy at the selected scale from the signal when applying wavelet transform. In Fig. 10, five wavelet candidates are applied and their coefficient energy after wavelet transform at fourth level was computed and compared.

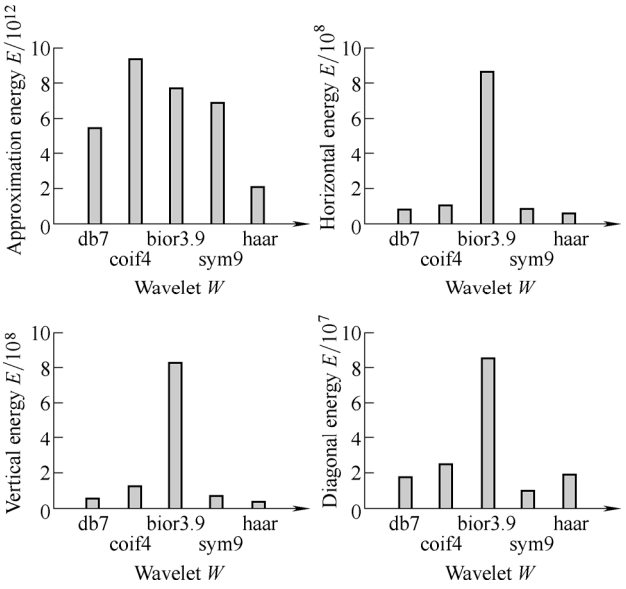

Fig. 10. Coefficient energy comparision of approximation and details use different wavelet

As can be seen from the Fig. 10, the maximum coefficient energy of approximation is obtained by coif4, while the energy of coif4, bior3.9, sym9 are all relatively large. In addition, the directional coefficient energy distribution of high frequency behaves different. The high frequency coefficient energy of bior3.9 wavelet in horizontal, vertical, diagonal direction are all much larger than the others. This means the bior3.9 wavelet is highly approximating to extract related component in the signal.

Tabel 1 shows an example of the reconstruction results of the fourth level using the five different wavelet methods for comparison. From Table 1 it can be concluded that the wavelet selection can also influence the results. Db7, coif4 and sym9 wavelet can effectively separate fibre information from the thermal image and reveal the impact point in the low frequency component. Fibre information in different direction was extracted and illustrated in H4, V4 and D4, respectively. However, it can be seen from the image that the impact point cannot be seen clearly. The reconstruction images using haar wavelet is blurred, that is because in mathematics, the haar wavelet is a sequence of rescaled square-shaped functions. Therefore, this phenomenon is most likely due to little similarities in shape between haar wavelet and the components in the thermal image. While bior3.9 wavelet performs the best, which not only separate high frequency component related to fibre information, but also reveal the impact point which fully retain the low frequency component as can be seen clearly in the enlarged

Tabel 1. Reconstruction results comparision of the fourth level use different wavelets

Coif 4	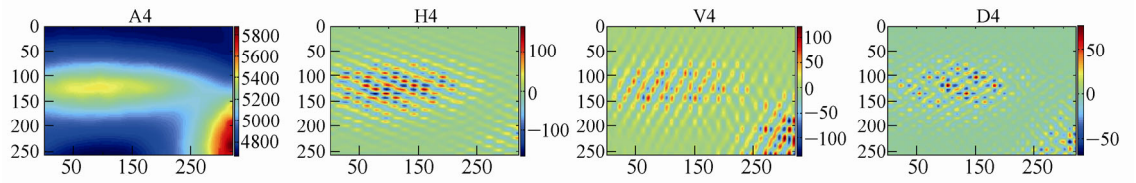			
Db7	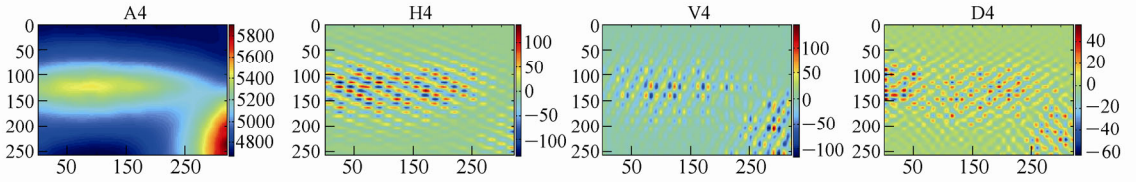			
Bior3.9	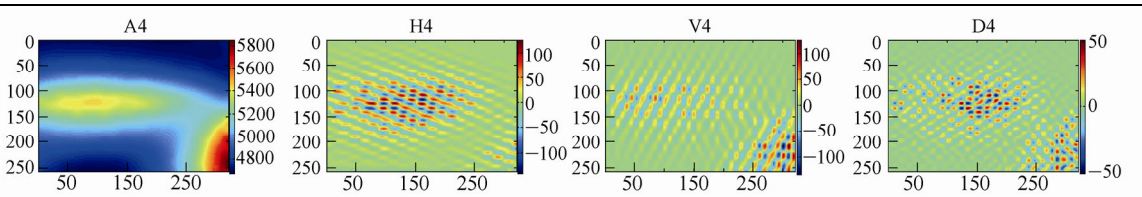			
Haar	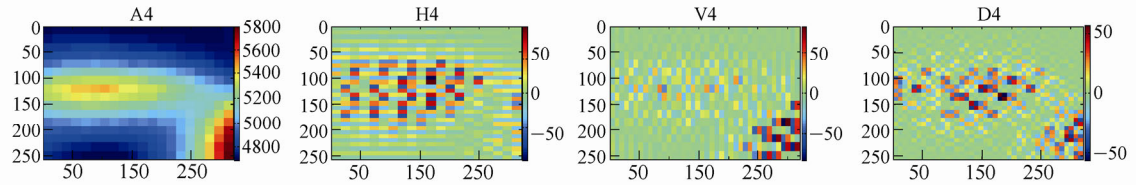			
Sym9	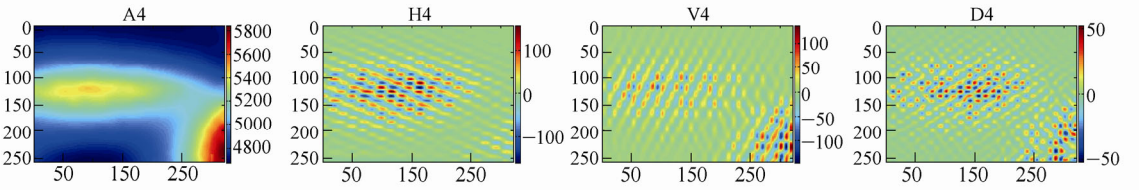			

image in Fig. 11. Moreover, the optimal wavelet may vary from one application to another based on the nature or shape of the signal.

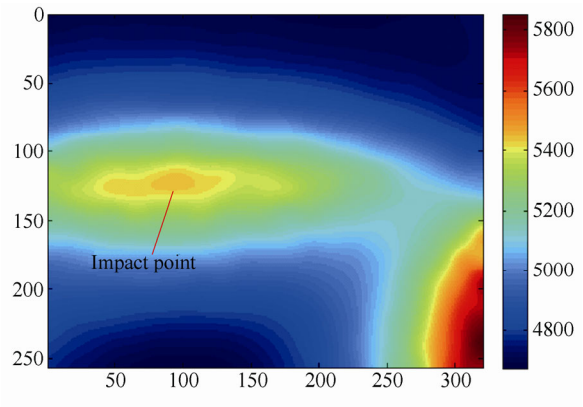

Fig. 11. Enlarged approximation of fourth level using bior3.9 wavelet

4 Conclusions

(1) According to the frequency component analysis by using the wavelet coefficient energy driven approach, an automatic method for optimal transient frame selection from thermal sequences is proposed. The thermal image at the end of heating stage is selected as optimal frame.

(2) Through dividing ECPT thermal image signal into different frequency subbands using wavelet transform, low energy impact damage is revealed from the ECPT thermal image and fibre texture is detected through proper scale selection.

(3) Optimized base wavelet is selected and investigated. The wavelet analysis based optimization process can be applied to further quantitative NDE of ECPT for different conductive material inspection.

The qualitative and quantitative criteria will be investigated in the later study through analyzing the samples impacted by different impact energy.

References

[1] CHAND S. Review carbon fibers for composites[J]. *Journal of Materials Science*, 2000, 35(6): 1303–1313.

[2] GARNIER C, PASTOR M L, EYMA F, et al. The detection of aeronautical defects in situ on composite structures using non-destructive testing[J]. *Composite Structures*, 2011, 93(5): 1328–1336.

[3] ZHOU Zhenggan, LIU Siming. Nonlinear ultrasonic techniques used in nondestructive testing：A review[J]. *Journal of Mechanical Engineering*, 2011, 47(8): 2–11. (in Chinese)

[4] YAN Bingsheng, LIU Ziran, ZHANG Yuechun, et al. Experimental study of early fatigue nonlinear ultrasonic detection in magnesium alloy[J]. *Journal of Mechanical Engineering*, 2013, 49(4): 20–24.

[5] YANG Binfeng, LUO Feilu, PAN Mengchun. Identification of corrosion fringe in pulsed eddy current nondestructive testing[J]. *Chinese Journal of Mechanical Engineering,* 2008, 44(12): 75–79. (in Chinese)
[6] TIAN Guiyun, SOPHIAN A. Reduction of lift-off effects for pulsed eddy current NDT[J]. *NDT & E International*, 2005, 38(4): 319–324.
[7] KORDATOS E Z, AGGELIS D G, MATIKAS T E. Monitoring mechanical damage in structural materials using complimentary NDE techniques based on thermography and acoustic emission[J]. *Composites Part B: Engineering*, 2012, 43(6): 2676–2686.
[8] LIU Junyan, TANG Qingju, LIU Xun, et al. Research on the quantitative analysis of subsurface defects for non-destructive testing by lock-in thermography[J]. *NDT & E International*, 2012, 45(1): 104–110.
[9] LI Guohua, WU Lixin, WU Miao, et al. Current status and applications of infrared thermography[J]. *Infrared and Laser Engineering*, 2004, 33(3): 227–230.
[10] GHASR M T, ABOU-KHOUSA M, KHARKOVSKY S, et al. Portable real-time microwave camera at 24 GHz[J]. *IEEE Trans. Antennas and Propagation*, 2012, 60(2): 1114–1125.
[11] WANG Qi, CHEN Zhiqiang, WU Xiaoping, et al. Review of X-ray security inspection technology[J]. *Computerized Tomography Theory and Applications*, 2004, 13(1): 32–37.
[12] EGBERT A. X-ray nanoCT of electronic components: Visualizing of internal 3D-structures with submicrometer resolution[C]// *Electronics System-Integration Technology Conference*, Greenwich, UK, September 1–4, ESTC, 2008: 399–402.
[13] TIAN Guiyun, HE Yunze, ADEWALE I, et al. Research on spectral response of pulsed eddy current and NDE applications[J]. *Sensors and Actuators A: Physical*, 2013, 189: 313–320.
[14] WILSON J, TIAN Guiyun, ABIDIN I Z, et al. Modelling and evaluation of eddy current stimulated thermography[J]. *Non-destructive Testing and Evaluation*, 2010, 25(3): 205–218.
[15] WILSON J, TIAN Guiyun, ABIDIN I Z, et al. Pulsed eddy current thermography: system development and evaluation[J]. *Insight-Non-Destructive Testing and Condition Monitoring*, 2010, 52(2): 87–90.
[16] WEEKES B, ALMOND D P, CAWLEY P, et al. Eddy-current induced thermography-probability of detection study of small fatigue cracks in steel, titanium and nickel-based super alloy[J]. *NDT & E International*, 2012, 49: 47–56.
[17] ZENZINGER G, BAMBERG J, SATZGER W, et al. Thermographic crack detection by eddy current excitation[J]. *Non-destructive Testing and Evaluation*, 2007, 22(2–3): 101–111.
[18] WILSON J, TIAN Guiyun, MUKRIZ I, et al. PEC thermography for imaging multiple cracks from rolling contact fatigue[J]. *NDT & E International*, 2011, 44(6): 505–512.
[19] ADEWALE I D, TIAN Guiyun. Decoupling the influence of permeability and conductivity in pulsed eddy current measurements[J]. *IEEE Transaction on Magnetics*, 2013, 49(3): 1119–1127.
[20] GUO Xingwang, VAVILOV V, SHIRYAEV V. Thermal nondestructive testing of corrosion in aviation aluminum panels and data processing algorithms[J]. *Journal of Mechanical Engineering*, 2009, 45(3): 208–214. (in Chinese)
[21] MARINETTI S, GRINZATO E, BISON P G, et al. Statistical analysis of IR thermographic sequences by PCA[J]. *Infrared Physics & Technology*, 2004, 46(1–2): 85–91.
[22] RAJIC N. Principal component thermography for flaw contrast enhancement and flaw depth characterization in composite structures[J]. *Composite Struct.*, 2002, 58: 521–528.
[23] KHAN A A, VRABIE V, MARS J I, et al. A source separation technique for processing of thermometric data from fiber optic DTS measurement for water leakage identification in dikes[J]. *IEEE Sensors Journal*, 2008, 8(7): 1118–1129.
[24] GAO Bin, BAI Libing, TIAN Guiyun, et al. Automatic defect identification of eddy current pulsed thermography using single channel blind source separation[J]. *IEEE Transactions on Instrumentation and Measurement*, 2014, 63(4): 913–922.
[25] REN Wenwei, LIU Jia, TIAN Guiyun, et al. Quantitative non-destructive evaluation method for impact damage using eddy current pulsed thermography[J]. *Composites Part B: Engineering*, 2013, 54: 169–179.
[26] HE Yunze, PAN Mengchun, LUO Feilu. Defect characterization based on heat diffusion using induction thermography testing[J]. *Rev. Sci. Instrum*, 2012, 83: 104702-1–104702-10.
[27] CHENG Liang, TIAN Guiyun. Pulsed electromagnetic NDE for defect detection and characterization in composites[C]//*IEEE International Instrumentation and Measurement Technology Conference*, Graz, AUT, May 13–16, 2012: 1902–1907.
[28] BUI H K, GUILLAUME W, DIDIER T, et al. 3-D modeling of thermo inductive non destructive testing method applied to multilayer composite[J]. *IEEE Transactions on Magnetics*, 2013, 49(5): 1949–1952.
[29] GUO Xingwang, LV Zhenxia, GAO Gongchen. Image reconstruction and enhancement of pulsed infrared thermography of CFRP laminates[J]. *Infrared Technology*, 2006, 28(5): 299–305.
[30] KAMBOH A M, RAETZ M, OWEISS K G, et al. Area-power efficient VLSI implementation of multichannel DWT for data compression in implantable neuroprosthetics[J]. *IEEE Transaction on Biomedical Circuits and Systems*, 2007, 1(2): 128–135.
[31] CHANG SG, YU B, VETTERLI M. Adaptive wavelet thresholding for image denoising and compression[J]. *IEEE Transactions on Image Processing*, 2000, 9(9): 1532–1546.
[32] ARIVAZHAGAN S, GANESAN L. Texture classification using wavelet transform[J]. *Pattern Recognition Letters*, 2003, 24(9–10): 1513–1521.
[33] HLAWATSCH F, AUGER F. Time-frequency analysis[M]. Great Britain: Antony Rowe Ltd, Chippenham, Wiltshire, 2010.
[34] CHENG Liang, TIAN Guiyun. Transient thermal behaviour of eddy-current pulsed thermography for non-destructive evaluation of composites[J]. *IEEE Transactions on Instrumentation and Measurement*, 2013, 62(5): 1215–1222.

Biographical notes

YANG Hailong, born in 1988, is currently a master candidate at *School of Automation Engineering, University of Electronic Science and Technology of China, Chengdu, China.* His research interests include instrument science and non-destructive testing and evaluation.
E-mail: yanghailong9889@163.com

GAO Bin, born in 1983, is currently an associate professor at *School of Automation Engineering, University of Electronic Science and Technology of China, Chengdu, China.* He received his PhD degree from *Newcastle University*. His main research interests include sensors, signal processing, machine learning, data mining for non-destructive testing and evaluation.
E-mail: bin_gao@uestc.edu.cn

TIAN Guiyun, born in 1965, is currently a professor and a PhD candidate supervisor at *School of Electrical and Electronic Engineering, Newcastle University, UK*. He received his PhD degree from *University of Derby, Derby, UK,* in 1998. Currently, he is "The Thousand Talents" professor with the *School of Automation Engineering, University of Electronic Science and Technology of China*. His mainly research interests include electromagnetic sensors, sensor array and sensor network, electromagnetic non-destructive testing and evaluation, advanced signal processing monitoring systems and applications.
E-mail: g.y.tian@newcastle.ac.uk

REN Wenwei, born in 1968, is currently a teacher at *School of Automation Engineering, University of Electronic Science and Technology of China, Chengdu, China.* Her main research interests include material science and non-destructive testing and evaluation.
E-mail: kgwrww@uestc.edu.cn

WOO Wailok, born in 1972, is currently an associate professor and a PhD candidate supervisor at *School of Electrical and Electronic Engineering, Newcastle University, UK*. He is the director of *Operations for the International Branch of the University*, and head of *the Machine Learning Centre for Sensing and Signal Processing*. His research interests include intelligent systems and algorithms, sensing and signal processing for non-destructive testing and evaluation.
E-mail: Lok.Woo@newcastle.ac.uk